Theoretical study of the enhanced Brønsted acidity of Zn^{2+}-exchanged zeolites

Luis A.M.M. Barbosa and Rutger A. van Santen

Schuit Institute of Catalysis, Laboratory of Inorganic Chemistry and Catalysis, Eindhoven University of Technology, PO Box 513, 5600 MB Eindhoven, The Netherlands

Received 7 June 1999; accepted 21 September 1999

The effect of Zn^{2+} exchange on the Brønsted acidity of a protonic zeolite has been studied by the *ab initio* DFT (density functional theory) approach using the BLYP generalized gradient approximation. Three different zeolite cluster models have been compared: two 6“T” models (two 4“T” rings with an oxygen atom bridge) with Si/Al = 1 and Si/Al = 2 and a 4“T” model (ring form) with Si/Al = 1. The Brønsted acidity has been probed by computation of the acetonitrile adsorption and the cluster deprotonation energy. The presence of Zn^{2+} does not affect the cluster Brønsted acidity but it creates a very strong Lewis site (Zn^{2+}) in all models studied. On the other hand, the presence of $ZnOH^+$ enhanced the Brønsted site acidity in the case of the 6T model with Si/Al = 1. This enhancement is due to a change in cluster geometry and position of OH group in $ZnOH^+$ upon acetonitrile adsorption.

Keywords: *ab initio*, Zn^{2+}, $ZnOH^+$, zeolites, Brønsted site and Lewis site acidity

1. Introduction

Protonic zeolites have been shown theoretically [1] as well as experimentally [2] to be weaker than superacids. A recent *in situ* NMR study of carbenium ion formation indicated that zeolite protons appear to be not stronger than an 80% sulfuric acid solution [2b].

On the other hand, the presence of Lewis sites is claimed to enhance the acid strength of their neighbor Brønsted sites [3] and it has been proposed that this synergetic interaction may result in superacidic behavior [4]. For instance, dealumination of zeolites, which creates deposits of extra-framework aluminum (EFAl) – AlO or $AlOH^+$ – has been shown to increase the Brønsted acidity in many different reactions. Disproportionation of toluene [4], isobutane/2-butene alkylation [5], isomerization and hydration of α-pirene [6], ethylbenzene hydroisomerization [7] and MTBE synthesis in the gas phase [8] are just few examples. Promoters such as alkali cations (Li^+, Na^+ or Rb^+) [9] and adsorbed Lewis acid (BF_3) on H-EMT zeolite [10] have been shown to increase similarly the acid strength.

It is also known that low-coordination transition metal cations (Zn^{2+}, Ga^{3+} and Cd^{2+} among others), which are stabilized in the voids of zeolites, exhibit Lewis-acid properties and are believed to be the active sites for a variety of catalytic conversion reactions [11].

For instance, zeolites containing Zn, Ga and Cd cations have been reported to catalyze dehydrogenation of small paraffins such as ethane [12], aromatization of *in situ* generated ethylene [13], aromatization of propane [11b], as well as hydration of acetylene [14]. Zinc is well known to be the active site in enzymes for hydration of CO_2 in living organisms and in many other human tissues, such as the red blood cells [15]. One example of those enzymes is *carbonic anhydrase* that catalyses conversion of CO_2 to $[HCO_3]^-$ [16].

The Brønsted acidity of Ga–H-ZSM-5, prepared via impregnation, does not show any great alteration compared to the H-ZSM-5. The concentration of strong acidic sites appears to be only weakly dependent on Ga content [12,17]. Unlike Ga–H-ZSM-5, Zn-containing H-ZSM-5 undergoes a large change in acidity; the amount of strong acid sites decreases by introducing Zn cations via ion exchange and impregnation [12a,b]. Lower Brønsted acidity has been observed when pentasils [17a], ZSM-22 [16b], MCM-22 [17c] or Y (Si/Al = 5) [17d] are modified by exchanging protons by Zn^{2+}. The total number of Brønsted sites decreases while the Lewis sites number increases [17a]. It has been demonstrated that Zn^{2+} exchanges with protons of strong acidic OH groups of the zeolite.

The effect of Zn^{2+} exchange on neighbor Brønsted site acid strength of the zeolite has been studied theoretically in the present work. Three different cluster models are used (figure 1 and table 1): two 6“T” models (two 4“T” rings with an oxygen atom bridge) with Si/Al = 1 and Si/Al = 2 and a 4“T” model (ring form) with Si/Al = 1. Different aspects were examined: the effect on Brønsted site strength, the formation of different Lewis sites (Zn^{2+} and $ZnOH^+$), and cluster geometry. A comparison between the strength of Brønsted and Lewis acid sites is also provided.

Acetonitrile was chosen as a probe molecule as it has previously been successfully applied in either theoretical [18] or experimental [19] studies. Considerable computational time is also saved when a small basic molecule is used rather than pyridine, etc.

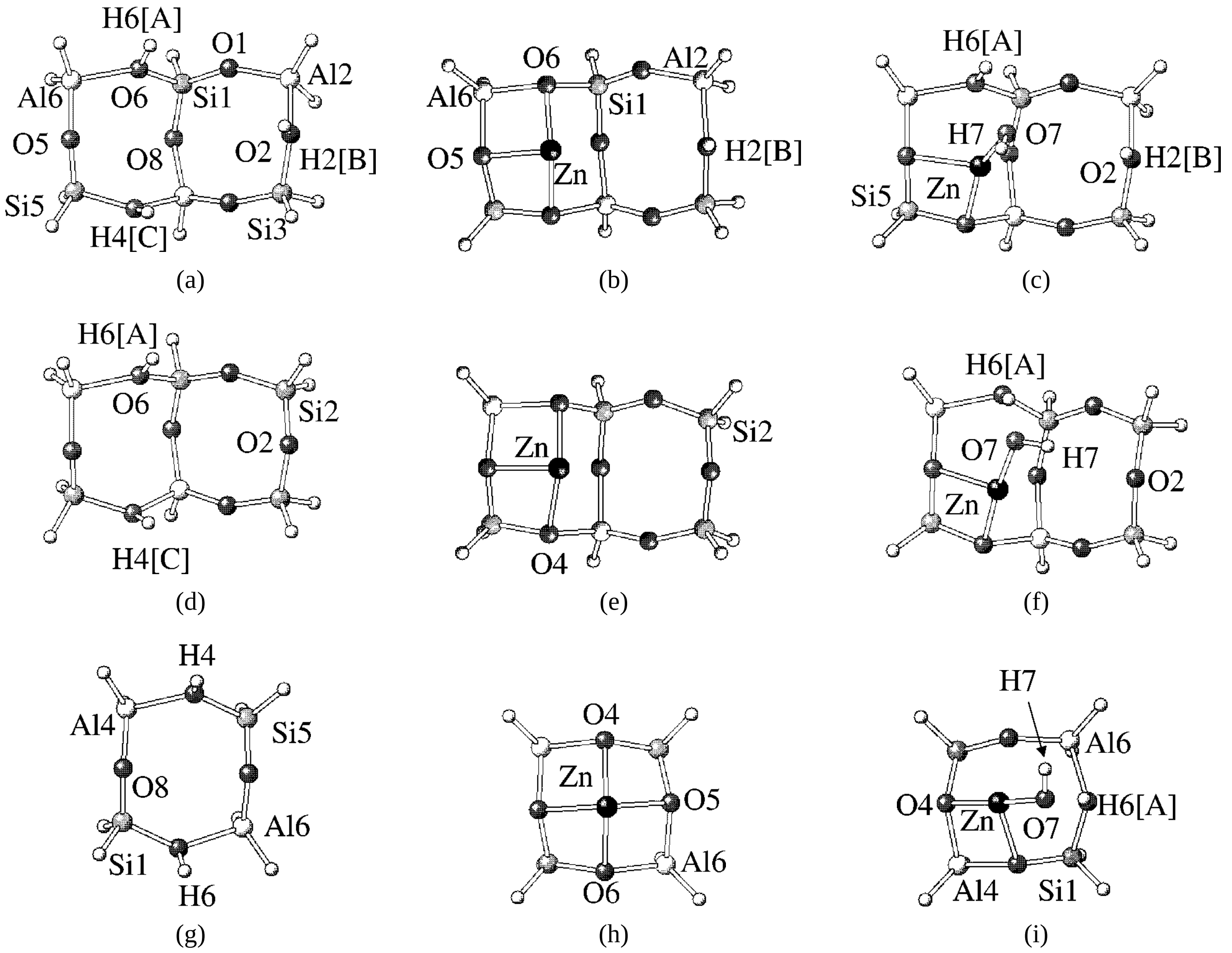

Figure 1. Cluster models and different Brønsted sites.

Table 1
Description of the models.

Code	Model
6T	6T model (Si/Al = 1) – figure 1(a)
6T-nit	6T model (Si/Al = 1) with acetonitrile adsorbed
6TZn	6T model (Si/Al = 1) with Zn^{2+} – figure 1(b)
6TZn-nit	6T model (Si/Al = 1) with Zn^{2+} with acetonitrile adsorbed – figure 2
6TZnOH	6T model (Si/Al = 1) with (ZnOH)$^{+}$ – figures 1(c) and 3
6TZnOH^{1}	6T model (Si/Al = 1) with (ZnOH)$^{+}$ – figure 3
6TZnOH^{2}	6T model (Si/Al = 1) with (ZnOH)$^{+}$ – figure 4
6TZnOH^{3}	6T model (Si/Al = 1) with (ZnOH)$^{+}$ – figure 6
6TZnOH-nit	6T model (Si/Al = 1) with (ZnOH)$^{+}$ with acetonitrile adsorbed – figures 3 and 4
6TZnOH2-nit	6T model (Si/Al = 1) with (ZnOH)$^{+}$ with acetonitrile adsorbed – figure 6
6TSi	6T model (Si/Al = 2) – figure 1(d)
6TSiZn	6T model (Si/Al = 2) with Zn^{2+} – figure 1(e)
6TSiZnOH	6T model (Si/Al = 2) with (ZnOH)$^{+}$ – figures 1(f) and 5
6TSiZnOH^{1}	6T model (Si/Al = 2) with (ZnOH)$^{+}$ – figure 5
6TSiZnOH^{2}	6T model (Si/Al = 2) with (ZnOH)$^{+}$ – figure 7
6TSiZnOH-nit	6T model (Si/Al = 2) with (ZnOH)$^{+}$ with acetonitrile adsorbed – figure 5
6TSiZnOH2-nit	6T model (Si/Al = 2) with (ZnOH)$^{+}$ with acetonitrile adsorbed – figure 7
4T	4T model (Si/Al = 1) – figure 1(g)
4TZn	4T model (Si/Al = 1) with Zn^{2+} – figure 1(h)
4TZnOH	4T model (Si/Al = 1) with (ZnOH)$^{+}$ – figure 1(i)
4TZnOH-nit 4TZnOH2-nit	4T model (Si/Al = 1) with (ZnOH)$^{+}$ – figure 7

2. Methods

In the present work a 6T fragment cluster (a connection of two small rings with 4 T atoms) is used to model the zeolite frame (see figure 1(a)). A 6TSi cluster model, which is the 6T model in which Al(2) has been replaced by a Si atom (see figure 1 (a) and (d)) and a 4T fragment, a small ring that contains the equal number of Al and Si atoms (see figure 1(g)) have been used. The initial geometries were taken from the faujasite X-ray results available in the Insight II package.[1]

All models have two neighboring Brønsted acid sites. These are required in order to exchange divalent cations [11b,12,17]. The choice of H-terminated Si groups rather than OH-terminated groups is to avoid intramolecular hydrogen bonds, which would result in the creation of an unacceptable model [20].

It has been previously shown that the cluster approach provides qualitatively meaningful results. Activation energies are typically 10 kJ/mol higher than those found for extrapolated bulk zeolite reactions. The use of such approach has been extensively discussed elsewhere [20,21].

All calculations have been performed using DZVP (double-zeta valence plus polarization function) for all atoms. This basis set is designed to provide double-ζ quality for importance valence region and a single function to represent the less chemically reactive core orbital [22]. This basis set incorporates polarization function in all atoms, excepting hydrogen atoms. A second auxiliary basis set (A1) was also used to expand the electron density in a set of a single-particle Gaussian-type functions [23] typically used by default in the DGauss[2] package code [24]. The choice of large basis set, double-ζ type, has been shown to give good accuracy in energy predictions and in geometry configurations [25].

Density functional theory (DFT) has been used in this study. The Becke exchange energy [26] plus Lee–Yang–Parr correlation functional [27] (BLYP) have been employed. These functionals give acceptable values for molecular energies and reasonable values for geometries [25].

Frequency calculations were performed in order to verify the stationary point geometries. These tests result in no imaginary frequencies, which indicates that these stationary points were local minima [28].

All energies were corrected using zero-point energy (ZPE). The chosen basis set was previously optimized for use in order to minimize the basis set superposition error (BSSE), as suggested by Radzio et al. [29].

No symmetry constraints have been used for any of the configurations studied. The exception is the 4T ring (figure 1(g)), where the oxygen atom (O8) was fixed in the "up" position to be compared to the substituted cluster (figure 1 (h) and (i)).

3. Results and discussion

The adsorption energy of acetonitrile on Brønsted and Lewis acid sites has been calculated using different Zn^{2+}-exchanged clusters. Also, the proton affinity of the neighboring Brønsted site has been computed. Three different proton positions can be distinguished: [A], [B] and [C] in our models (see figure 1(a)). The cluster nomenclature code used in the current work is described in table 1.

3.1. The position of the Zn^{2+} cation in the cluster model

Zn^{2+} cations sit in the double-four ring inside of the cage. This supercage position was found by Seidel et al., when zinc ions were incorporated in Y zeolites by chemical vapor deposition and reaction (CVDR) method [30].

The Zn^{2+} cation is tetracoordinated to oxygen atoms from the framework as follows from studies with zeolite A [31], sodalite [31] and ZSM-5 [11b]. In our case, the Zn^{2+} cation is tetracoordinated to the oxygen atoms in the 4T ring model (see figure 1(h)) but not in the 6TZn and 6TSiZn models (figure 1 (b) and (e)). The main difference is the position of the oxygen O8. The "up" position (closer to the cation) was found to be preferred in the 4T ring, while the "down" position was preferred in the 6TZn and 6TSiZn models (see O8–Zn distance in the table 2). The average distance between the Zn^{2+} cation and the oxygen atoms was about 1.97 and 2.09 Å in the study with sodalite and zeolite A [31] and ZSM-5 [11b], respectively. This agrees with the average values found here for 6T and 4T models, 2.08 and 204 Å, respectively.

Interestingly, unlike the Co^{2+} coordination to a six-ring in zeolites [32], the Zn^{2+} cation settles out of the plane of the oxygen atoms of the 6T and 4T model studied here. In both cases, the Zn cation experienced a steric hindrance effect because of the small size of cluster even if the models have some geometric distortions after the cation loading.

3.2. Effect of Zn^{2+} exchange on Brønsted site strength

Comparing the 6T, 6TZn, 6TSi and 6TSiZn models (figure 1 (a), (b), (d) and (e)), one can see that the total number of protons decreases after Zn^{2+} exchange: the Brønsted sites [A] and [C] (figure 1 (a) and (d)) are substituted by the Zn cation. The acetonitrile adsorption energies, as well as the deprotonation energies calculated on those sites are shown in table 3. In the case of Si/Al ratio equal to 2 (6TSi) those Brønsted sites are equivalent but they have slightly different strength for the ratio equal to 1 (6T).

The Brønsted site [B] is the proton left after Zn^{2+} cation exchange (see figure 1(b)). In the original cluster (6T

---

[1] Insight II – Catalysis 3.0 Biosym/MSi, 9685 Scranton Road, San Diego, CA 92121-3752, USA.

[2] DGauss program, version 2.1, part of Unichem package from Cray Research Inc.

Table 2
Optimized model geometries, distances in Å.

	Model											
	6T	6TZn	6TZnOH	6TSi	6TSiZn	6TSiZnOH	4TZn	4TZnOH	6T-nit	6TZn-nit	6TZnOH-nit	6TSiZnOH-nit
Site [B]												
O2–Al2	2.03	2.04	2.02	–	–	–	–	–	1.98	2.01	–	–
O2–H2	0.98	0.98	0.98	–	–	–	–	–	1.01	1.00	–	–
O2–Si3	1.76	1.76	1.77	1.69	1.69	1.69	–	–	1.75	1.75	–	–
O2–Si2	–	–	–	1.66	1.66	1.66	–	–	–	–	–	–
Al(O2)Si	127.9°	135.9°	134.1°	–		–	–	–	–	–	–	–
Si(O2)Si	–	–		137.0°	141.5°	–	–	–	–	–	–	–
O2AlO1Si	−78.5°	−77.3°	−77.4°	–	–	–	–	–	–	–	–	–
O2SiO1Si	–	–		−64.8°	127.9°		–	–	–	–	–	–
							–	–	–	–	–	–
Site [C]												
Al4–O4	1.96	–	–	1.96	1.92	–	1.93	–	–	–	–	–
O4–H4	0.98	–	–	0.99	–	–	–	–	–	–	–	–
Si5–O4	1.78	–	–	1.77	1.72	–	1.70	–	–	–	–	–
Site [A]												
Al6–O6	1.98	–	2.01	2.00	2.00	1.99	–	2.00	1.96	–	–	–
O6–H6	0.98	–	0.99	0.98	–	1.02	1.69	1.03	1.00	–	–	–
O6–Si1	1.78	–	1.80	1.76	1.72	1.75	1.69	1.75	1.75	–	–	–
Site Zn												
O4–Zn	–	2.01	2.05	–	2.00	2.01	2.07	2.03	–	–	–	–
O5–Zn	–	2.13	2.27	–	2.16	2.22	2.09	2.31	–	–	–	–
O6–Zn	–	1.97	2.61	–	1.98	2.96	–	2.80	–	–	2.71	–
O7–Zn	–	–	1.84	–	–	1.85	–	1.87	–	–	–	–
O7–H7	–	–	0.98	–	–	0.98	–	0.98	–	–	–	–
O8–Zn	–	2.28	2.51	–	2.31	2.49	2.09	2.24	–	–	–	–
O7–H2	–	–	3.64	–	–	–	–	–	–	–	1.63	–
O7–H6	–	–	2.6	–	–	1.84	–	1.78	–	–	3.46	3.16
O2–H8	–	–	–	–		3.00					–	2.51

model) the acetonitrile interaction energy with this proton is −43.2 kJ/mol. A new value is calculated when acetonitrile interacts with this Brønsted site [B] in the 6TZn model: −39.8 kJ/mol. The acid strength of this site is comparable to the original value (see table 3). This is also confirmed by the proton affinity: 1236.3 kJ/mol for 6TZn[B] and 1236.5 kJ/mol for 6T model.

The acid strength of the zeolite is revealed by the degree of interaction of the base (acetonitrile) with the Brønsted site. This interaction promotes an electron donor–acceptor transfer within the zeolite frame to compensate for the proton donation. Mortier [33] proposed that this electron donor–acceptor transfer results in a shortening of Al–O and Si–O bonds of the Brønsted site. Comparing the 6T/6T-nit and 6TZn/6TZn-nit models (see table 2 for the site [B]), one can see these bonds lengths decrease by 0.04 and 0.01 Å, respectively. All these results indicate that the Brønsted site strength is not enhanced after Zn^{2+} ion exchange.

At higher coverage of acetonitrile (using model 6TZn), an interesting effect appears. The interaction with the Brønsted site decreases by approximately 12.3 kJ/mol. Acetonitrile adsorbed in the Brønsted site suffers a steric repulsion from the other acetonitrile molecule. The angle C–N–H8 changes from 170.6° at low to 168.5° at high coverage, as well as the angle N–H2–O2 from 178.8 to 177.2° and the distance between N–H2 from 1.95 to 1.85 Å, respectively (see figure 2). At high coverage, the nitrogen lone-pair orbital cannot perfectly overlap with the hydrogen s atomic orbital.

3.3. Adsorption on the Lewis site

A new Lewis site is formed (Zn^{2+}) when protons are exchanged. This site will compete with the remaining Brønsted sites for acetonitrile adsorption. To study this competition the interaction of acetonitrile with this Lewis site was calculated. The computed adsorption energy is, respectively, −125.6 (6TZn), −131.5 (6TSiZn) and −125.5 kJ/mol (4TZn). These values are very close, because they correspond to a similar cluster environment for the Zn^{2+} cation (see figure 1 (b), (e) and (h)). Comparison with the values previously obtained for the interaction with the Brønsted sites reveals that acetonitrile will preferentially adsorb on the Lewis site Zn^{2+}, as the energy is lowered.

Experimental results of pyridine adsorption, using zeolite Y with Si/Al ratio equal to 6.6 [17d], also indicate that a considerable Lewis acidity is created after Zn^{2+} exchange accompanied by a decrease in Brønsted acidity.

At higher coverage of acetonitrile (using model 6TZn), the same steric repulsion occurs. The interaction energy of acetonitrile with the Lewis site decreases by the same value (ca. 12.3 kJ/mol) as mentioned for the Brønsted site. The

Table 3
Acetonitrile adsorption and proton affinity energies (kJ/mol).

	Model									
	6T	6TZn	6TZnOH	6TZnOH^{1,2}	6TSi	6TSiZn	6TSiZnOH	6TSiZnOH^{1,2}	4TZn	4TZnOH
Acetonitrile adsorption energy on Lewis site ZnOH$^+$	–	–	−89.4		–	–	−71.6	–	–	−8.1 −72.9(2)
Acetonitrile adsorption energy (using the distorced geometry)	–	–	–	−34.9^1	–	–	–	−58.7^2	–	
Acetonitrile adsorption energy on Brønsted site	−29.5[A] −43.2[B] −36.3[C]	−39.8[B]	−87.9[A] −48.0[B]	−31.6[A]^1 −39.2[B]^2	−34.6[A] −35.6[C]	–	−24.9[A]	−24.3[A]^1	–	−22.3
Acetonitrile adsorption energy on Brønsted site Co-adsorbed with a second acetonitrile on Lewis site	–	−27.5[B]	–	–	–	–	–	–	–	–
Acetonitrile adsorption energy on Lewis site Zn^{2+}	–	−125.6	–	–	–	−131.5	–	–	−125.5	–
Acetonitrile adsorption energy on Lewis site Co-adsorbed with a second acetonitrile on Brønsted site	–	−113.3	–	–	–	–	–	–		–
Proton affinity	1269.4[A] 1236.5[B] 1233.2[C]	1236.3[B]	1154.2[A] 1220.3[B]	1272.6[A]^1 1240.3[B]^2	1245.5[A] 1241.4[C]	–	1209.1[A]	1209.5[A]^1	–	1207.5

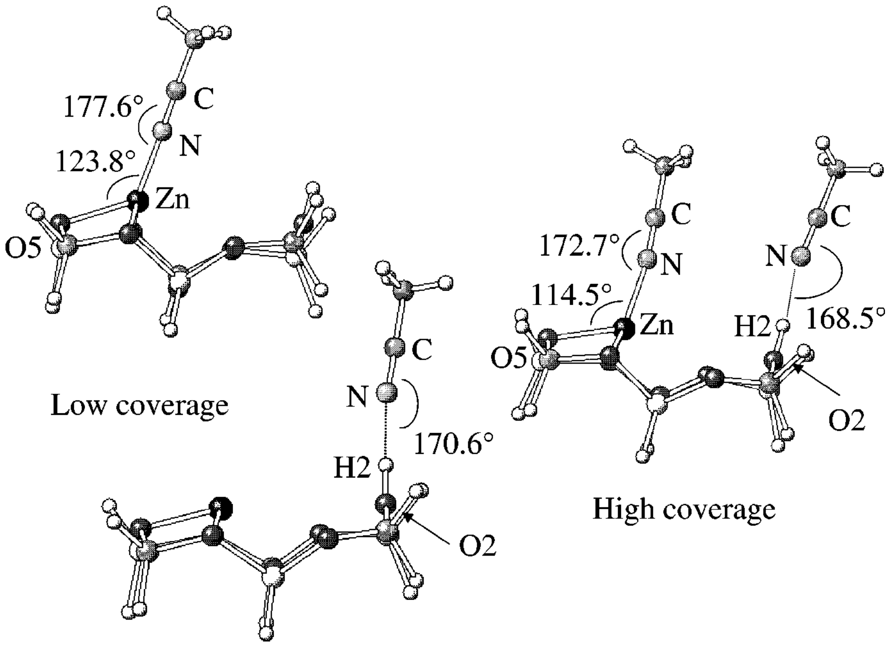

Figure 2. Acetonitrile adsorption in different degree of coverages.

angle N–Zn–O5 changes from 123.8° at low to 114.5° at high coverage, as well as the angle C–N–Zn from 177.6 to 172.7°, respectively (see figure 2). At high coverage, the nitrogen lone-pair orbital also cannot perfectly overlap the zinc s atomic orbital.

3.4. Effect of formation of ZnOH$^+$ Lewis site

It has been shown in the previous section that Zn^{2+} is a strong Lewis acid. When water is in contact with Zn^{2+}-exchanged zeolite [34], it will physically adsorb

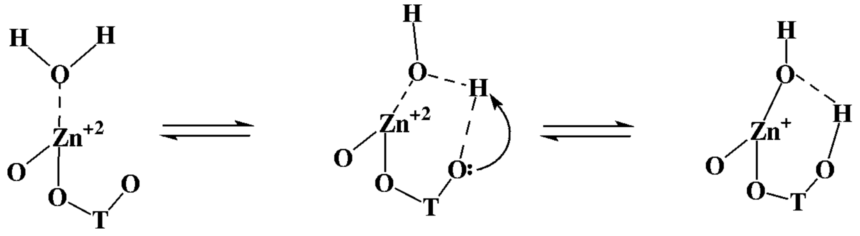

Scheme 1. Dissociation of water on Zn^{2+}-containing zeolite.

to this Lewis site and may heterolytically cleave (see scheme 1) forming a new Brønsted site and a new Lewis site $ZnOH^+$ [11b]. In our models this new acid site has the same relative position as the previous Brønsted site [A] (see figure 1(c)). The synergetic effect of the Lewis site ($ZnOH^+$) on the Brønsted site strength has also been studied by using the three different cluster models.

3.5. $ZnOH^+$ effect on the Brønsted site strength

3.5.1. Si/Al = 1: Brønsted site [A] and [B] – model 6TZnOH

In figure 3, the optimized geometries for two different models are shown: 6TZnOH, 6TZnOH-nit. The first model corresponds to the initial cluster geometry and the second model to the cluster geometry after acetonitrile adsorption. It can be seen for the first two models that orientation of the OH group of the Lewis site changes, by moving away from its original position.

Prior to acetonitrile adsorption, the OH group forms a hydrogen bond with proton H6 (distance O7–H6 is 2.60 Å, see figure 3: 6TZnOH). This hydrogen bond is broken when acetonitrile interacts with the proton (H6); the OH group moves away because of the repulsive interaction with acetonitrile, changing the distance O7–H6 from 2.60 (6TZnOH) to 3.46 Å (6TZnOH-nit). The OH group moves towards the proton H2, inducing distortions in the cluster (see 6TZnOH-nit in figure 3) and creating a new and stronger H bond: O7–H2 (1.63 Å). These cluster distortions were also observed in similar studies [35] using different monovalent cations (Li^+, Na^+, K^+, $Ca(OH)^+$, AlO^+ and $Al(OH)_2^+$) substituted in zeolite clusters (6T with Si/A = 1). In this work analogous H-bond formation between the Lewis and Brønsted site has been formed when calculations were performed with $Al(OH)_2^+$.

The new cluster configuration (6TZnOH-nit model without acetonitrile interaction: see figure 3 – 6TZnOH^1) has been optimized. The new O7–H6 and O7–H2 distances are 3.80 and 1.62 Å, respectively, indicating that the distortions remain. The proton affinity for site [A] is 1272.6 kJ/mol, compared with 1154.2 kJ/mol for the original 6TZnOH cluster. This new value for the proton affinity shows that those configurations are not equivalent.

The acetonitrile interaction energy, calculated using these different cluster configurations, shows an interesting result: −87.9 kJ/mol using the original geometry (6TZnOH) and −34.9 kJ/mol using the second geometry (6TZnOH^1).

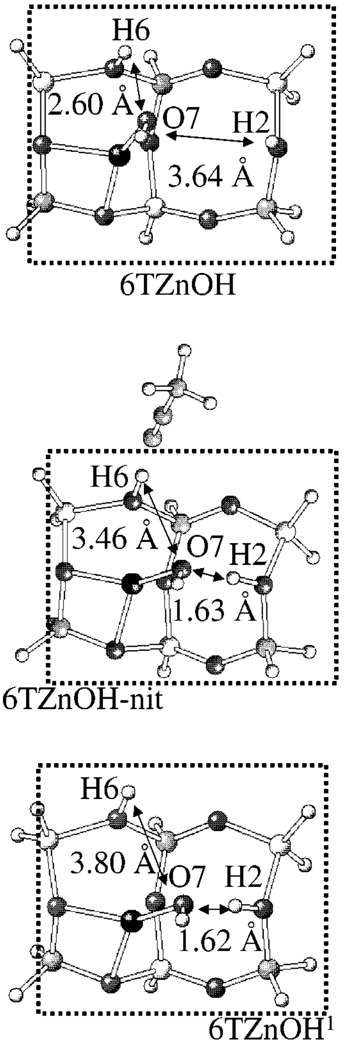

Figure 3. Cluster geometry distortion for the model 6TZnOH (Brønsted site [A]).

With $ZnOH^+$ present, the Brønsted acid strength is found to be enhanced by the cluster distortions (compare the values in table 3 for 6T[A], [B] and [C] with 6TZnOH[A]). Makarova et al. [10] found similar enhancement on H-EMT after low-temperature adsorption of BF_3 and claimed that on the basis of the theoretical calculations an amphoteric interaction between the Lewis acid (BF_3) and the zeolite results, which enhances the acidity of the remaining uncomplexed Brønsted hydroxyls. Recently, experimental studies with cations substituted on clays also

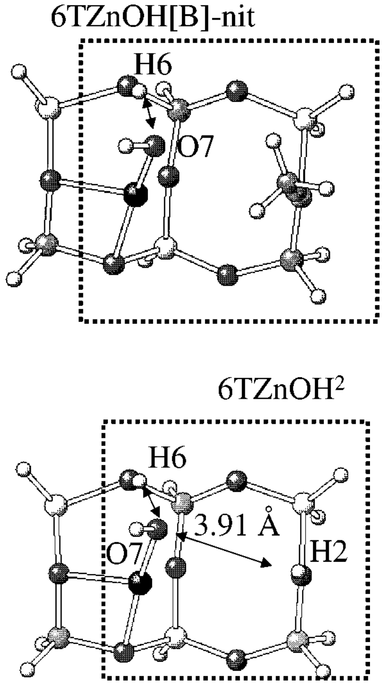

Figure 4. Cluster geometry distortion for the model 6TZnOH (Brønsted site [B]).

show that Zn^{2+}-containing clays have stronger acidity than other substituted clays samples when compared via the acetonitrile interaction [36].

For the other Brønsted site [B], no repulsion between acetonitrile and the OH group of the ZnOH$^+$ site is observed. Therefore there are no strong distortions in the cluster geometry. Optimizing the new cluster configuration (6TZnOH[B]-nit cluster without interaction with acetonitrile: figure 4 – 6TZnOH^2), the H6–O7 distance changes slightly from the original value (6TZnOH) 2.60 to 1.91 Å and H2–O7 distance from 3.64 to 3.91 Å, respectively. Without strong geometry changes (hydrogen bond formation between O7 and H2), the adsorption energy remains almost the same: -48.0 (6TZnOH) and -39.8 kJ/mol (6TZnOH^2), as well as the deprotonation energy of those cluster models: 1220.3 and 1240.3 kJ/mol (see table 3). The stronger these geometry changes (H-bond formation), the higher the energy difference.

3.5.2. *Si/Al = 2 and Brønsted site [A]*

This model (6TSiZnOH) has only one Brønsted site, which is formed after the water OH bond cleavage. The Brønsted site has the same relative position in the cluster as the previous Brønsted site [A]. In figure 5, one can see the optimized geometries of two different models: 6TSiZnOH, 6TSiZnOH-nit. The first model corresponds to the initial cluster geometry and the second model to the cluster geometry after acetonitrile adsorption. When acetonitrile interacts with the Brønsted site [A], as previously seen (Si/Al = 1 ratio), the hydrogen bond H6–O7 is broken and the OH group moves towards the O2 atom (see figure 5: 6TSiZnOH and 6TSiZnOH-nit). Therefore it creates some distortions in the cluster.

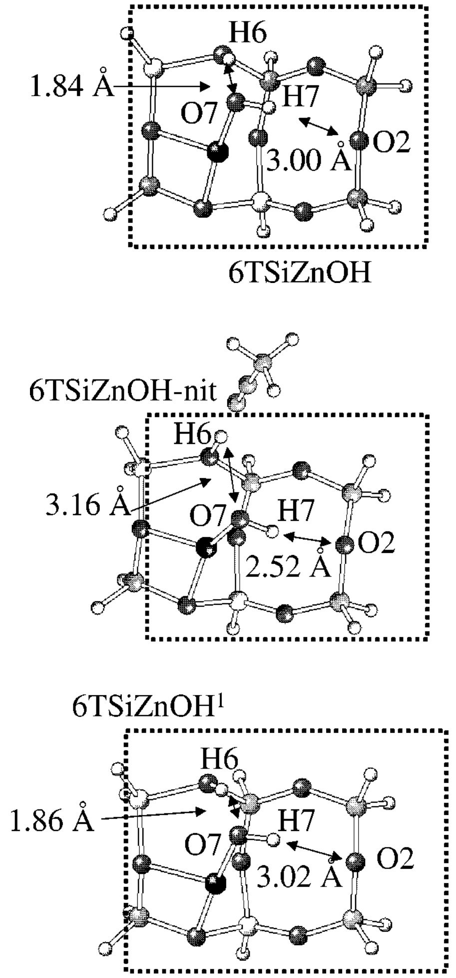

Figure 5. Cluster geometry distortion for the model 6TSiZnOH (Brønsted site [A]).

When we optimize the new cluster geometry (cluster 6TSiZnOH-nit without interaction with the acetonitrile: figure 5 – 6TSiZnOH^1), these distortions disappear and the distances H7–O2 and H6–O7 return almost to their original values: 3.00 and 1.84 Å, respectively. Therefore no large differences are found between the acetonitrile interaction energies calculated using either 6TSiZnOH or 6TSiZnOH^1: -24.9 and -24.3 kJ/mol, respectively (see table 3). The same energy value was found when a smaller cluster (4TZnOH model – figure 1(i)) is used: -22.3 kJ/mol; which also does not have geometric distortions.

The strength of the new Brønsted site (from 6TSiZnOH) decreases, the computed interaction energy differs by 10 kJ/mol from its original value (protonic cluster 6TSi), because there is neither distortion nor H-bond (H7–O2) formation on the final cluster geometry, see table 3. A similar result has been obtained for the strength of Brønsted site in the 4TZnOH cluster, in which the computed interaction energy is reduced by 17.2 kJ/mol from its original value (39.6 kJ/mol in protonic cluster 4T).

3.6. Adsorption on Lewis site ZnOH$^+$

3.6.1. Si/Al = 1

The acetonitrile adsorption on the new Lewis site ZnOH$^+$ has also been studied. In figure 6, one can see the optimized structure of the cluster in contact with acetonitrile (6TZnOH2-nit). Without acetonitrile adsorption, as we have seen previously, the OH group forms an H bond with the proton H6. Clearly, the 6TZnOH2-nit model shows that acetonitrile forces the OH group (by acetonitrile repulsion) to move away. The new distance O7–H6 is now 4.70 Å and the OH group moves again towards the proton H2. This induces distortions in the cluster model and also creates a new and stronger H bond: O7–H2 (1.45 Å). These cluster distortions have already been observed when acetonitrile interacted with the Brønsted site [A].

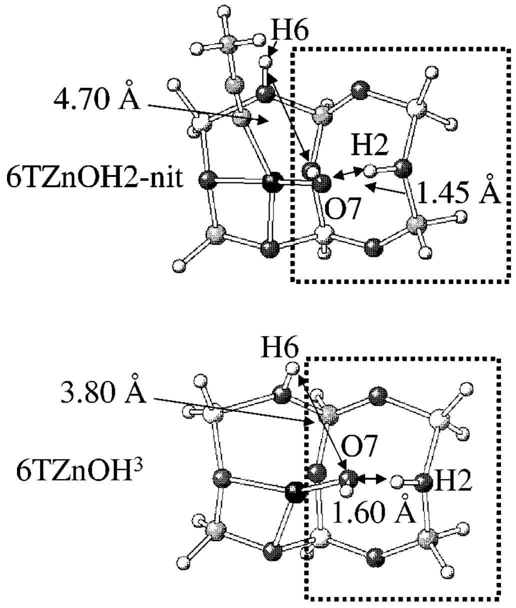

Figure 6. Cluster geometry distortion for the model 6TZnOH (Lewis site ZnOH$^+$).

This new cluster configuration (6TZnOH2-nit without acetonitrile) has also been optimized, but the deformations remained. The new O7–H6 and O7–H2 distances are 3.80 and 1.60 Å, respectively (see figure 6 – 6TZnOH^3). The optimized clusters, 6TZnOH^3 and 6TZnOH^1, have almost the same final structures, thus we will consider those structures as the same.

The acetonitrile interaction energies calculated using these different configurations (6TZnOH and 6TZnOH^1) show again an interesting result: -89.4 kJ/mol using the original geometry (6TZnOH) and -34.9 kJ/mol using the distorted one (6TZnOH^1). As in the previous section, the acetonitrile interaction energy increases, when the O7–H2 hydrogen bond is formed, compared to the original 6TZnOH model. In the present case, the energy difference is the same as found for the Brønsted site [A]: -54.5 and -56.3 kJ/mol, respectively.

3.6.2. Si/Al = 2

Similarly to our previous calculations, in figure 7, the optimized geometry of the system 6TSiZnOH2-nit (acetonitrile interacting with Lewis site ZnOH$^+$) shows that the OH group moves away from its original position (figure 5 – 6TSiZnOH). In this case, instead of going only towards the O2 atom, the OH moves also closer to H6 atom. The distance between H7–O2 changes from 3.00 (6TSiZnOH) to 2.00 Å (6TSiZnOH2-nit) and from 1.84 to 1.41 Å for the O7–H6 bond, respectively, creating again some distortions in the cluster.

The distance H7–O2 is not restored, compared to its original value 3.00 Å, even after the new cluster geometry optimization (6TSiZnOH-nit cluster without acetonitrile interaction: figure 7 – 6TSiZnOH^2). The H7–O2 and O6–H7 distances change to 2.64 and 1.72 Å, respectively. The

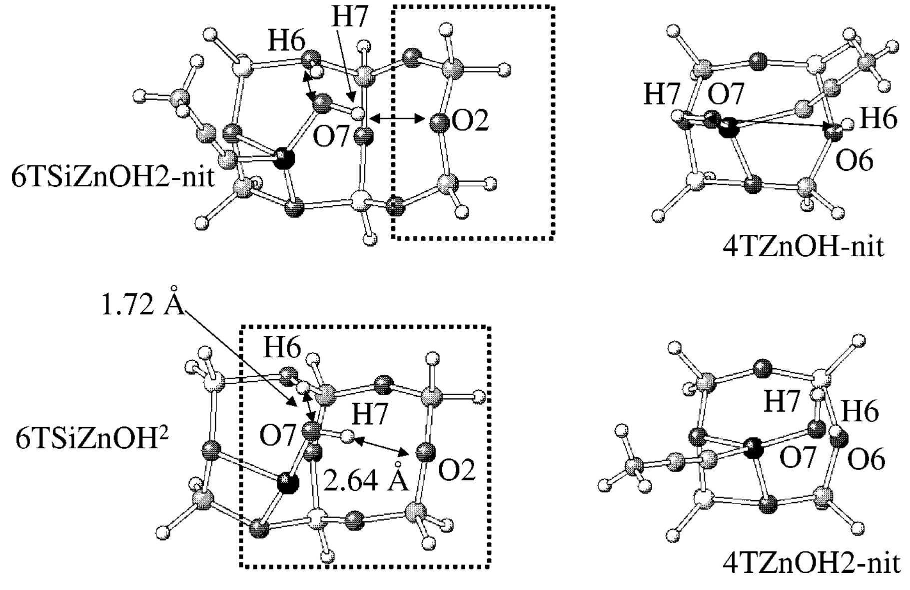

Figure 7. Cluster geometry distortion for 6TSiZnOH and 4TZnOH models (Lewis site ZnOH$^+$).

cluster still contains some distortions, therefore some differences in acetonitrile interaction energies are found for both 6TSiZnOH and $6TSiZnOH^2$ cluster models: -71.6 and -58.7 kJ/mol, respectively (see table 3). Interestingly, the acetonitrile pushes the OH group towards the H2 atom, but the H bond formed (H2–O7) is still strong in the absence of acetonitrile, due to the basic character of the OH group of $ZnOH^+$ site.

Using small cluster models (4T – figure 7), the influence of H-bond creation/cleavage process is also noticed. There are two different possibilities of interaction between acetonitrile and $ZnOH^+$ (4TZnOH-nit and 4TZnOH2-nit, figure 7). The main difference is the H bond (H6–O7). While in the configuration 4TZnOH-nit, acetonitrile breaks this H bond (see figure 1(i) – 4TZnOH), in the configuration 4TZnOH2-nit, the acetonitrile forces the OH group to move towards H6, forming a strong bond in 4TZnOH2-nit. This result is reflected directly in the interaction energy: -8.1 kJ/mol for the 4TZnOH-nit model and -72.9 kJ/mol for the 4TZnOH2-nit (see table 3). The latter interaction energy value is in complete agreement with the previous one found for the 6TSiZnOH.

4. Conclusions

No increase in Brønsted acid strength is found for Zn^{2+}-exchanged zeolite. The Zn^{2+} ion interacts more strongly with acetonitrile than a zeolitic proton, indicating that acetonitrile preferentially adsorbs at this Lewis site. At higher acetonitrile coverages (in the $Si/Al = 1$, 6TZn model – figure 2), steric repulsion between two acetonitrile molecules decreases slightly the interaction energy.

The $ZnOH^+$ models show an interesting effect. Acetonitrile experiences a repulsive interaction with the OH group from the Lewis site. This forces the OH to move towards the O2 position, which corresponds to the proton [B] position (see clusters 6TZnOH-nit, 6TZnOH2-nit and 6TSiZnOH) or the O6 position, which corresponds to the proton [A] position (6TSiZnOH2-nit), thus creating distortions in the final cluster geometry. Due to a H-bond cleavage/formation process, the Brønsted acidity of those protons is now enhanced. Changes in the size and the Si/Al ratio of the models confirm our observations. Typical examples are found for the 6TZnOH and 4TZnOH models.

It is well known that acetonitrile is protonated in superacid solutions, such as FSO_3H–SBF_5–SO_2 [37]. However, no indication of acetonitrile protonation is found in the final optimized configuration for our enhanced acidity cases. This indicates that superacidity could not be achieved by the presence of $ZnOH^+$ or by Zn^{2+}.

Acknowledgement

LAMMB thanks the National Council of Scientific and Technologic Development (CNPq, Brazil) for the scholarship and National Computing Facilities Foundation (NCF, The Netherlands) for the computational resources under the project SC-475. This work has been performed under auspices of NIOK, the Netherlands Institute for Catalysis Research, Lab. Report No. TUE-99-5-05.

References

[1] (a) G.J. Kramer and R.A. van Santen, J. Am. Chem. Soc. 115 (1993) 2887;
(b) G.J. Kramer and R.A. van Santen, Chem. Rev. 95 (1995) 637.

[2] (a) V. Addeeva, J.W. de Haan, J. Jänchen, G.D. Lei, V. Schünemann, L.J.M. van de Ven, W.M.H. Sachtler and R.A. van Santen, J. Catal. 151 (1995) 364;
(b) J.F. Haw, J.B. Nicholas, T. Xu, L.W. Beck and D.B. Ferguson, Acc. Chem. Res. 29 (1996) 259.

[3] C. Mirodatos and D. Barthomeuf, J. Chem. Soc. Chem. Commun. 2 (1981) 39.

[4] N.P. Rhodes and R. Rudha, J. Chem. Soc. Faraday Trans. 90 (1994) 809.

[5] (a) A. Corma, A. Martinez and C. Martinez, Appl. Catal. A 134 (1996) 169;
(b) A. Corma, A. Martinez, P.A. Arroyo, J.L.F. Monteiro and E.F. Souza-Aguiar, Appl. Catal. A 142 (1996) 139.

[6] (a) A. Severino, A. Esculcas, J. Rocha, J. Vital and L.S. Lobo, Appl. Catal. A 142 (1996) 255;
(b) H. Valente and J. Vital, in: *Heterogeneous Catalysis and Fine Chemicals IV*, eds. H.U. Blaser, A. Baiker and R. Prins (Elsevier, Amsterdam, 1997) p. 555.

[7] L.D. Fernandes, J.F. Monteiro, E.F. Souza-Aguiar, A. Martinez and A. Corma, J. Catal. 177 (1998) 363.

[8] A. Nikolopoulos, A. Kogelbauer, J.G. Goodwin, Jr. and G. Marcelin, Appl. Catal. A 119 (1994) 69.

[9] A. Nikolopoulos, A. Kogelbauer, J.G. Goodwin, Jr. and G. Marcelin J. Catal. 148 (1994) 157.

[10] M.A. Makarova, S.P. Bates and J. Dwye, J. Am. Chem. Soc. 117 (1995) 11309.

[11] (a) I.E. Maxwell, Adv. Catal. 31 (1982) 1;
(b) J.A. Biscardi, G.D. Meitzner and E. Iglesia, J. Catal. 170 (1998) 192.

[12] (a) Y. Ono, Catal. Rev. Sci. Eng. 34 (1992) 179;
(b) B.S. Quake and W.M.H. Sachtler, J. Catal. 145 (1994) 456;
(c) M.V. Frash and R.A. van Santen, J. Phys. Chem., submitted;
(d) M.V. Frash and R.A. van Santen, Phys. Chem. Chem. Phys., submitted.

[13] A. Hagen and F. Roessener, in: *Studies in Surface Science and Catalysis*, Vol. 98, eds. H.G. Krager and J. Weitkamp (Elsevier, Amsterdam, 1995) p. 189.

[14] (a) G.Y. Onyestyák and D. Kalló, in: *Catalyst Deactivation*, Studies in Surface Science and Catalysis, Vol. 34, eds. B. Delmont and G.F. Froment (Elsevier, Amsterdam, 1987) p. 605;
(b) G.Y. Onyestyák, J. Papp and D. Kalló, in: *Zeolites as Catalysts, Sorbents and Detergent Builders*, Studies in Surface Science and Catalysis, Vol. 46, eds. H.G. Karge and J. Weitkamp (Elsevier, Amsterdam, 1989) p. 241;
(c) G.Y. Onyestyák and D. Kalló, in: *Catalysis by Microporous Materials*, Studies in Surface Science and Catalysis, Vol. 94, eds. H.K. Beuer, H.G. Karge, I. Kiricsi and J.B. Nagy (Elsevier, Amsterdam, 1995) p. 435;
(d) G.Y. Onyestyák and D. Kalló, Zeolites 17 (1996) 489;
(e) G.Y. Onyestyák and D. Kalló, J. Mol. Catal. A 106 (1996) 103.

[15] S. Lindskog, in: *Zinc Enzymes*, Vol. 1, eds. W. Maret and M. Zeppezamer (Birkhäuser, Boston, 1986) ch. 22.

[16] (a) A.E. Eriksson, P.M. Kylsten, T.A. Jones and A. Liljas, Proteins 4 (1988) 283;
(b) D. Lu and G. Voth, J. Am. Chem. Soc. 120 (1998) 4006;

(c) A. Vendani, D.W. Huhta and S.P. Jacober, J. Am. Chem. Soc. 111 (1989) 4075.

[17] (a) V.I. Yakerson, T.V. Vasina, L.I. Lafer, V.P. Sytnyk, G.L. Dykh, A.V. Mokhov, O.V. Bragin and Kh.M. Minachev, Catal. Lett. 3 (1989) 339;
(b) N. Kuman, L.E. Lindfors and R. Buggningsbacka, Appl. Catal. A 139 (1996) 189;
(c) N. Kuman and L.E. Lindfors, Appl. Catal. A 147 (1996) 175;
(d) P.A. Arroyo, E.F. Souza-Aguiar and J.L.F. Monteiro in: *202nd ACS National Meeting*, Vol. 36, New York, August 1991.

[18] (a) J.F. Haw, M.B. Hall, A.E. Alvarado-Swaisgood, E.J. Munson, Z. Lin, L.W. Beck and T. Howard, J. Am. Chem. Soc. 116 (1994) 7308;
(b) A.G. Pelmenschikov, R.A. van Santen, J. Jänchen and E. Meijer, J. Phys. Chem. 97 (1993) 11071.

[19] (a) J. Jänchen, M.P.J. Peeters, J.H.M.C. van Wolput, J.P. Wolthuizen, J.H.C. van Hooff and U. Lohse, J. Chem. Soc. Faraday Trans. 90 (1994) 1033;
(b) J. Jänchen, H. Stach, M. Busio and J.H.M.C. van Wolput, Thermochim. Acta 312 (1998) 33.

[20] J. Sauer, P. Ugliengo, E. Garrone and V.R. Saunders, Chem. Rev. 94 (1994) 2095.

[21] (a) R. Shah, J.D. Gale and M.C. Payne, J. Phys. Chem. B 101 (1997) 4787;
(b) R.A. van Santen, Catal. Today 38 (1997) 377.

[22] N. Godbout, J. Andzelm, E. Wimmer and D.R. Salahub, Canad. J. Chem. 70 (1992) 560.

[23] J. Andzelm, N. Russo and D.R. Salahub, Chem. Phys. Lett. 142 (1987) 169.

[24] J. Andzelm and E. Wimmer, J. Chem. Phys. 58 (1992) 1280.

[25] A.C. Scheiner, J. Baker and J.W. Andzelm, J. Comput. Chem. 18 (1997) 775.

[26] A.D. Becke, Phys. Rev. A 33 (1988) 3098.

[27] C. Lee, W. Yang and R.G. Parr, Phys. Rev. B 37 (1988) 785.

[28] H.B. Schlegel, in: *Ab Initio Methods in Quantum Chemistry,* Part I, Advances in Chemical Physics, Vol. LXVII, eds. I. Priogine and S.A. Rice (Wiley–Interscience, Chichester, 1987) p. 249.

[29] E. Radzio, J.W. Andzelm and D.R. Salahub, J. Comp. Chem. 6 (1985) 533.

[30] A. Seidel, F. Rittner and B. Boddenberg, J. Phys. Chem. B 102 (1998) 7176.

[31] L. Khouchaf, M.-H. Tuiler, M. Wark, M. Soulard and H. Kessler, Micropor. Mesopor. Mater. (1998) 20, 27.

[32] K. Pierloot, A. Delabie, C. Ribbing, A.A. Verberckmoes and R.A. Shooneydt, J. Chem. Phys. B 102 (1998) 10789.

[33] W.J. Mortier, in: *Proc. 6th International Conference on Zeolite*, eds. D. Olson and A. Bisio (Butterworths, Guildford, 1984) p. 734.

[34] A. Hagen, K.-H. Hallmeier, C. Hennig, R. Szargan, T. Inui and F. Roessner, in: *Catalysis by Microporous Materials*, Studies in Surface Science and Catalysis, Vol. 94, eds. H.K. Beuer, H.G. Karge, I. Kiricsi and J.B. Nagy (Elsevier, Amsterdam, 1995) p. 195.

[35] N.O. Gonzales, A.K. Chakraborty and A.T. Bell, Catal. Lett. 50 (1998) 135.

[36] M.T.G. Oostenbrink, M.K. Oudenhuijzen and D.C. Koningsberger, to be published.

[37] G.A. Olah and T.E. Kiovsky, J. Am. Chem. Soc. 90 (1968) 4666.